Article

Slow Pyrolysis of *Quercus cerris* Cork: Characterization of Biochars and Pyrolysis Volatiles

Umut Sen [1,*] , **Marta Martins** [2] , **Everton Santos** [2] , **Maria Amelia Lemos** [2] , **Francisco Lemos** [2] **and Helena Pereira** [1]

1   Forest Research Centre, School of Agriculture, University of Lisbon, Tapada da Ajuda,
    1349-017 Lisbon, Portugal
2   CERENA/Chemical Engineering Department, Instituto Superior Técnico, University of Lisbon,
    1049-001 Lisbon, Portugal
*   Correspondence: umutsen@isa.ulisboa.pt

Abstract: Waste cork granules of *Quercus cerris* bark were subjected to isothermal and non-isothermal slow pyrolysis. The heat of the reaction, as well as the yields and properties of biochar, bio-oil, and pyrolysis gas were investigated by thermogravimetric analysis, FT-IR, CHN elemental analysis, higher heating value (HHV) determinations, scanning electron microscopy (SEM), and gas chromatography (GC). The slow pyrolysis was carried out in a semi-batch reactor using an isothermal or a non-isothermal dynamic approach. The results demonstrated that isothermal or non-isothermal slow pyrolysis of cork is a slightly exothermic reaction that produces biochars. The elemental analysis results indicated that non-isothermally produced chars have similar fuel properties compared to isothermally produced chars. The FT-IR results showed that cork suberin undergoes a higher degree of degradation in isothermal chars and aromatization begins in the char structure. Bio-oils are also produced and they consist of C_5–C_{12} hydrocarbons with C_8 carbon compounds making up the main fraction. Lighter components, mainly C_1–C_2 hydrocarbons are collected in the gas phase. The overall results indicate a possible reduced-cost route for the production of cork-based biochars by using non-isothermal slow pyrolysis.

Keywords: waste cork; pyrolysis; biochar; bio-oil; bark

1. Introduction

In recent years, biomass utilization to produce chemicals and energy has received increased attention as a result of environmental and economic concerns and growing world-wide ecological awareness. The biorefinery concept was developed, in which alternative technologies are applied to obtain added-value products from the low-value biomass or biomass components in cascading or parallel processes in a way similar to petroleum refineries [1,2].

Thermo-chemical processes, such as pyrolysis and gasification, are among those that show high potential for biomass utilization. Pyrolysis is carried out in oxygen-free or oxygen-isolated environments at relatively mild temperatures to obtain biochars and bio-oils while gasification is carried out under partially oxidizing conditions at high temperatures to obtain producer gas [3,4]. Pyrolysis and gasification may also be integrated to obtain liquid drop-in fuels, such as the proposed *bioliqTM* process developed in Germany [5]. Slow pyrolysis is one of the simplest pyrolysis processes that may be carried out for producing biochars in conventional kilns using isothermal heating regimes at temperatures of approximately 400 °C. On the other hand, fast pyrolysis is carried out to produce bio-oils at moderate temperatures (approximately 500 °C) using higher heating rates as well as low vapor and solid residence times [6]. Although the effect of temperature on yields and composition of the pyrolysis products is well-known and has been studied by micro-scale thermogravimetric methods such as TGA-FT-IR, relatively little is known of the

combined effect of solid and vapor residence times and the pyrolysis temperature profile on pyrolysis product compositions at a larger scale. A simple approximation to study the combined effects of solid and vapor residence times is to design a hybrid pyrolysis process with a simultaneous simulation of a slow pyrolysis solid residence time and a fast pyrolysis vapor residence time. This is a different form of intermediate pyrolysis with the application of shorter vapor residence time and longer solid residence times [6]. In the hybrid design it is possible to study the effect of the temperature profile on biochar properties.

Most pyrolysis research has considered wood and wood residues as feedstock [7,8]. Barks are increasingly envisaged as biorefinery feedstock namely by including them into thermochemical platforms [9,10]. Barks are structurally and chemically more complex than wood, requiring particular attention regarding their characterization [11,12]. One of the special features is related with the presence of cork, which may be substantial in barks of some species [13]. One such example is the Turkey oak (*Quercus cerris* L.), that has a bark with a considerable proportion of cork, which has already been characterized in detail [14] and its valorization addressed by a pilot-scale fractionation [15]. The purpose of this study is to produce biochars from the currently not commercially utilized cork fraction of Turkey oak bark using a hybrid pyrolysis approach and analyze biochar properties as well as the yields of pyrolysis products, as an integrative path within a solid waste management perspective.

2. Materials and Methods

2.1. Materials

Quercus cerris cork samples were obtained from the outer bark of trees sampled in the South of Turkey. The bark samples were manually separated from the recently harvested trees. The cork fractions were separated from the bark and ground and sieved to a 60–80 mesh (177–250 μm) particle size, which was used in the pyrolysis experiments. The detailed chemical and anatomical characterizations of the raw material can be found elsewhere [14].

2.2. Methods

2.2.1. Isothermal and Non-Isothermal Slow Pyrolysis

A Schlenk-type glass reactor was designed for the pyrolysis experiments to guarantee air-free conditions inside the reactor (Figure 1). The reactor was inserted into the oven with insulators to prevent heat loss, flushed with nitrogen, and the oven-heating program was run. The cork samples were kept in a sample holder sphere outside the reactor and were introduced into the reactor by turning the down the sphere when the oven temperature reached 500 °C. Two types of runs were carried out to obtain the biochars: either the oven temperature was kept constant at 500 °C, or the power was cut to the oven and the reaction proceeded as non-isothermal with decreasing temperature during the following 60 min (Figure 2). The volatiles were immediately captured using a condenser and liquid collector above the reactor. Pyrolysis gas was captured, using a gas burette, at the exit of the condenser. The temperature inside the reactor was registered continuously through a thermocouple during the pyrolysis experiments. Blank runs were carried out to calibrate the reactor behavior.
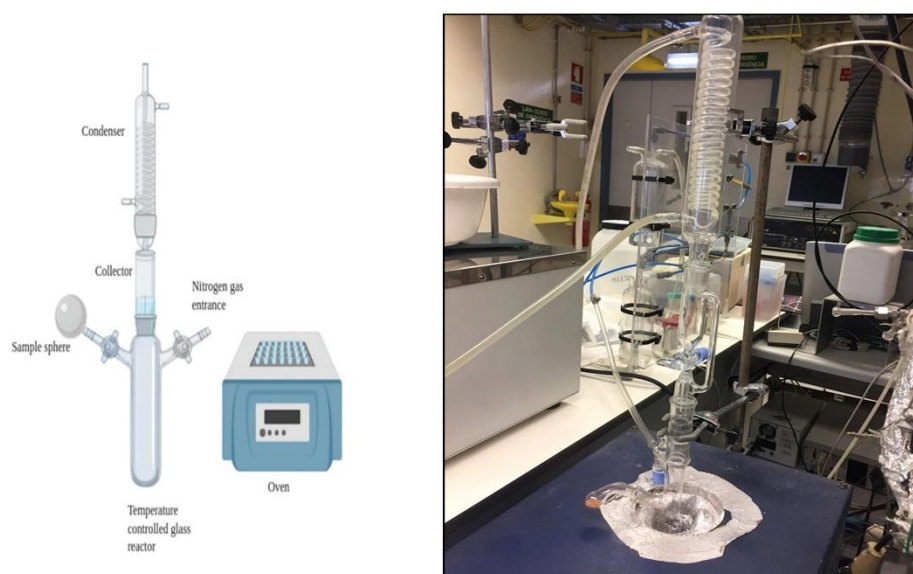
Figure 1. Schematics (**left**) of the Schlenk-type reactor used in the pyrolysis experiments (the figure was created with BioRender, www.biorender.com, accessed on 19 November 2022) (**left**), and photo (**right**) of the reactor before the sample introduction.
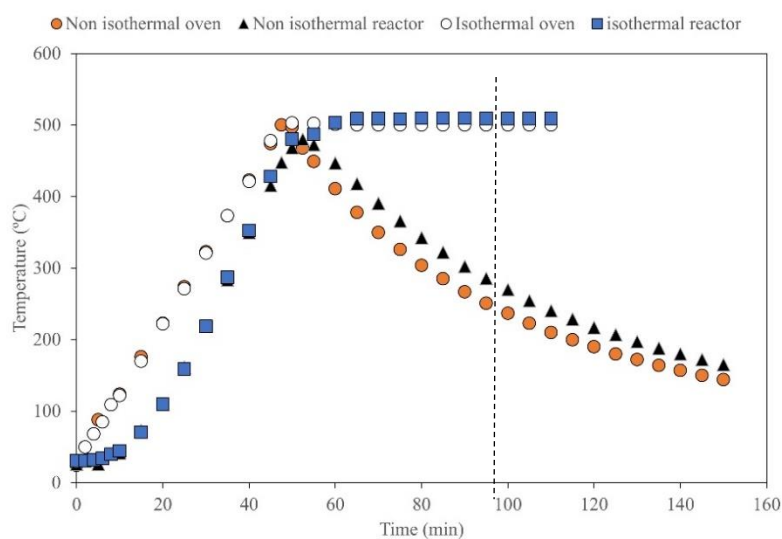
Figure 2. Temperature profiles in the oven (circles) and inside the reactor, in both isothermal and non-isothermal cases. The samples were introduced when the oven temperature reached 500 °C (vertical dashed-line).

During the heating phase, the temperature in the reactor was always lower than the oven temperature (Figure 2). After the reaction onsets, the reactor temperature is always higher than the oven. This is a clear indication that an exothermic reaction is occurring. To understand this effect, the heat flow to the reactor was analyzed. The chars produced by these two temperature profiles will be indicated hereafter as I-char for the isothermal profile and G-char for the non-isothermal one.

2.2.2. Differential Thermal Analysis of Reactor Operation

We used a differential thermal analysis approach to analyze the thermal effects in the laboratory scale reactor. Differential thermal analysis is a common way to analyze data in thermogravimetric equipment, in which the temperature difference between a sample and a reference material is measured as the temperature is increased.

Although it was not possible to have to exactly identical reactors, different experiments were performed with an empty reactor, used as reference, and the reactor containing the sample, at exactly the same heating temperature program. This allowed us to analyze the thermal aspects of the processes involved in the pyrolysis process in the two conditions.

2.2.3. Thermogravimetric Analysis

A Perkin Elmer STA 6000 simultaneous thermal analyzer was used to perform the thermogravimetric analysis (TGA) of biomass and biochar samples. A stepwise heating program was used: in the first step, approximately 10 mg of the 177–250 μm cork samples was kept isothermally at 30 °C for 10 min, followed by heating until 800 °C with heating rates between 10 and 200 °C min^{-1}. The cork or biochar samples were kept isothermal for 10 min and then cooled with a cooling rate of 50 °C min^{-1}. The nitrogen or air flow rates were set at 20 mL min^{-1} and alumina pans were used.

2.2.4. FT-IR Analysis

The cork and biochar samples (60–80 mesh particles) of *Quercus cerris* were placed on the diamond (ATR-FTIR) and the reflectance spectra were acquired with a Bruker FT-IR spectrometer in the range of 4000–400 cm^{-1} with a spectral resolution of 4 cm^{-1} [16].

2.2.5. Determination of Fuel Properties of Biochars

The fuel properties of isothermal and non-isothermal biochars were determined using proximate analysis, elemental analysis and higher heating value determinations. The proximate analysis was conducted with the thermogravimetric analyzer with application of nitrogen (pyrolysis) and air flow (combustion) modes. The moisture content and volatile matter data were obtained from the pyrolysis experiments. The ash content was obtained from the combustion experiments. The fixed carbon content was calculated by mass difference.

The elemental analysis consists of determinations of carbon and hydrogen contents according to M.M. 8.6 (A.E) (2009-05-06) standard using an elemental analyzer. The oxygen content was calculated by mass difference. The higher heating values (HHV) were measured according to CEN/TS 15400 Standard using a Parr oxygen bomb calorimeter.

2.2.6. Scanning Electron Microscopy

The char samples as well as the raw cork samples were analyzed with a scanning electron microscope (Hitachi TM3030Plus). The instrument was operated at 15 kV acceleration potential and a working distance of 1 mm.

2.2.7. Hydrocarbon Composition of Pyrolysis Volatiles

A Perkin Elmer Clarus 680 gas chromatograph was used to analyze hydrocarbon composition of previously toluene-extracted pyrolysis condensates and pyrolysis gas. The chromatograph is equipped with a flame ionization detector (FID) and an SGE BP1 capillary column 30 m long × 0.25 mm wide. The injector and detector temperatures were set to 340 °C during the experiment, and nitrogen was used as the carrier gas. The flow rates used in the detector were 45 cm^3 min^{-1} of hydrogen and 450 cm^3 min^{-1} of air, measured at atmospheric pressure and room temperature.

The following temperature program was used in the chromatograph: 2 min isothermal at 60 °C followed by heating at 10 °C min^{-1} until 190 °C, 5 min isothermal at 190 °C, heating at 10 °C min^{-1} until 200 °C, and finally isothermal at 200 °C for 60 min. The retention indexes of the hydrocarbon standards including n-ethane, 1-ethene, n-propane, 1-propene, n-butane, 1-butene, n-pentane, 1-pentene, 3-methylpentane, n-hexane, 1-hexene, n-heptane, 1-heptene, benzene, toluene, 2,2,4-trimethyl pentane, 1-octane, 2-methyl heptane, 1-nonene, n-decane, 1-decene, and n-dodecane were determined and the hydrocarbon components of bio-oils and pyrolysis gas were identified by retention time similarity.

3. Results

3.1. The Mass Balance

The mass yield of pyrolysis products is an important parameter for the economy of the pyrolysis process. Although the aim in slow pyrolysis is to produce biochars, secondary pyrolysis products, i.e., pyrolysis condensates and pyrolysis gas, may be important factors in the overall economy since these products may be used in the process or sold to produce materials or energy. In a conventional slow pyrolysis process, biomass undergoes thermal degradation at temperatures of approximately 400 °C for relatively short time (1–2 h) [6]. However, the exposure to isothermal heating during this period reduces the biochar yield, thereby reducing the process efficiency. The application of different temperature profiles such as non-isothermal pyrolysis may overcome this problem.

The mass yields of non-isothermal and isothermal pyrolysis are presented in Table 1. The results show that under the applied conditions, non-isothermal pyrolysis resulted in similar biochar and slightly lower condensate yields than isothermal pyrolysis. The mass yields in pyrolysis depend on a number of different factors such as pyrolysis conditions (temperature, heating rate, residence time), the reactor configuration (fixed-bed, fluidized bed, etc.), and the feedstock properties (chemical composition, particle size, moisture content, ash content, etc.). The higher heating rates applied to smaller biomass particles with high polysaccharide contents favor the formation of volatiles, while slower heating rates applied to larger biomass particles with high lignin content favor the formation of char [12–14].

Table 1. Comparative mass yields of pyrolysis products (as-received basis) in isothermal and non-isothermal pyrolysis.

Products (%)	Isothermal Pyrolysis	Non-Isothermal Pyrolysis
Biochar	32.3 ± 3.9	32.2 ± 15.8
Condensate	18.0 ± 6.3	16.7 ± 1.1
Gas	49.8 ± 2.4	51.2 ± 14.6

The gas yield was slightly higher in non-isothermal pyrolysis. The variation in pyrolysis product yields were also higher in non-isothermal pyrolysis. The overall reaction was slightly exothermic as can be verified from Figure 2 where the temperature of the reactor continued to increase after even after the heating was stopped at about 47 min. During the cooling, the reactor temperature was also higher than then the oven temperature. This result was interesting because even with an initial fast heat exposure, the overall reaction was exothermic.

The overall pyrolysis mass yields are similar to slow pyrolysis mass yields of other different lignocellulosic biomass species in the literature [6]. The condensate yield from cork was small, possibly due to insufficient heat transfer rate in the reactor. In fact, most industrial fast pyrolysis reactors use fluid bed technology, often including heat carrying materials, to guarantee higher heat transfer rates to produce bio-oils from lignocellulosic biomass.

3.2. Differential Thermal Analysis of Reactor Data

The temperature profile inside the reactor shows the temperatures to which the isothermal and non-isothermal chars were exposed (Figure 2). The isothermal char was exposed to 500 °C during most of the reaction while the non-isothermal char did not actually reach 500 °C due to the thermal lag between oven and reactor, and its temperature was reduced gradually after an initial increase. The sample temperature may be assumed as equal to the reactor temperature considering the small particle size of cork used in the experiments.

It has been argued that in biomass pyrolysis, temperature plays a more important role than solid residence time [17]. However, in most isothermal slow pyrolysis studies this effect was ignored, possibly because the main pyrolysis reactions occur during the heating period while the secondary reactions occur afterwards [18]. The non-isothermal pyrolysis

is likely to reduce the secondary reactions in decreasing temperatures due to the decreasing reaction rate constant as may be verified using the Arrhenius equation and could actually be considered as equivalent to a reduction in the residence time of the solid.

The biomass pyrolysis occurs via a series of simultaneous endothermic and exothermic reactions [19]. Different factors such as heating rate, biomass chemical composition, and catalytic reactions of pyrolysis vapours may affect the overall heat release [19,20]. The heat flow to the *Quercus cerris* cork samples during the slow pyrolysis reaction was estimated for the reactor experiments. The results demonstrated that the isothermal and non-isothermal slow pyrolysis of cork is a slightly exothermic reaction (Figures 3 and 4).
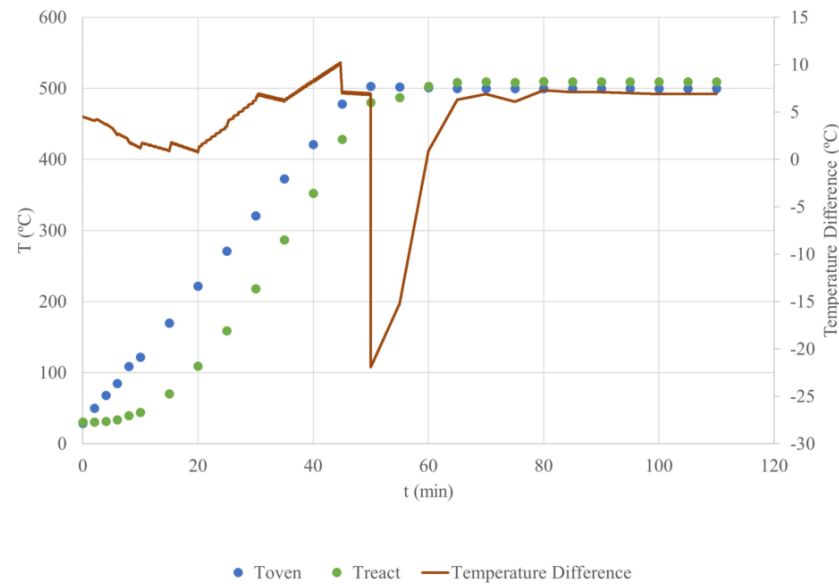
Figure 3. Temperature profile for the isothermal reactor containing the cork sample, corresponding temperature in the oven, and temperature difference between the reactor containing the sample and the empty reactor for the same temperature program.
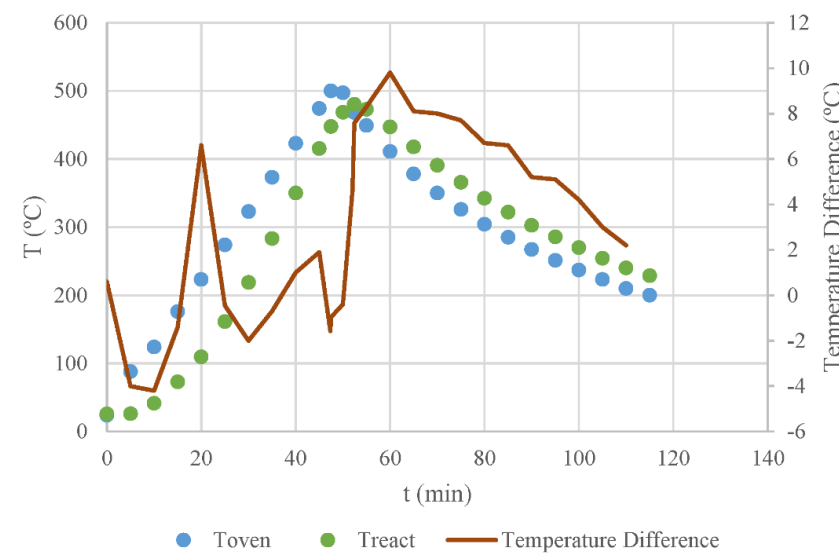

Figure 4. Temperature profile for the non-isothermal reactor containing the cork sample, corresponding temperature in the oven, and temperature difference between the reactor containing the sample and the empty reactor for the same temperature program.

3.3. The Effect of Temperature on the Surface Chemical Groups of Cork Biochars

The infra-red spectra show that temperature had a significant effect on the surface characteristics of cork biochars. A total of six prominent peaks may be detected on the raw cork which is in agreement with the previous reports [21–23]. The broad peak at approximately 3295 cm^{-1} is assigned to the O-H vibration and thus the moisture content of the cork. This peak almost disappears in the cork biochars (Figure 5), indicating that the biochars produced are essentially hydrophobic, although the non-isothermal char seems to retain some moisture. The peaks at 2921 and 2855 cm^{-1} are assigned to asymmetric and symmetric stretching vibrations of the methylene group of cork suberin, respectively. The intensity of peaks decreases significantly in non-isothermal chars and disappeared altogether in isothermal chars. The peak at 1738 cm^{-1} is assigned to C=O vibrations of carbonyl group of suberin and it also disappears in both cork biochars. These results show that suberin undergoes thermal degradation during the heat treatment which is in agreement with previous reports [23,24]. The peak at 1603 cm^{-1} is assigned to C-O stretching of calcium oxalate in cork [21,25]. The intensity of this peak was not changed in non-isothermal char but slightly reduced in isothermal chars. Possibly C=O stretching vibrations of cork lignin and hemicelluloses also contribute to the signals at 1738 cm^{-1} [26] and 1603 cm^{-1} [21,27]. The broad peak at 1031 cm^{-1} is assigned to the C-O vibrations of cork polysaccharides [21,28]. This peak disappears in cork biochars.
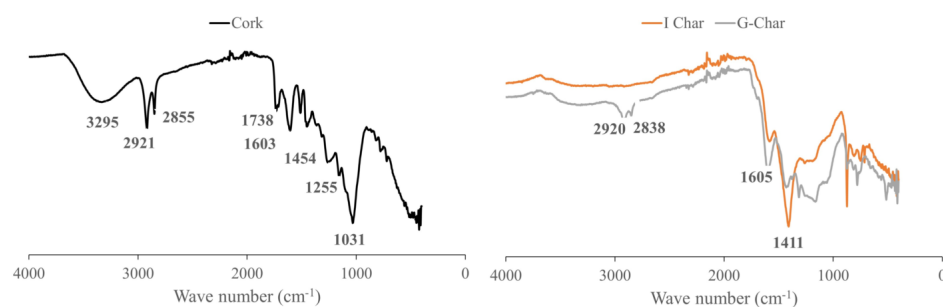
Figure 5. The effect of temperature on the surface groups of *Quercus cerris* cork (**left**) and *Quercus cerris* cork biochars (**right**).

3.4. The Morphology of Cork Biochars

The SEM micrographs of isothermal and non-isothermal biochars are shown in Figure 6. The cellular degradation in non-isothermal biochars is smaller than that of isothermal biochars. This result is in agreement with mass yields which indicate that increased extended exposure to heat in isothermal conditions results in a higher degradation in cork, possibly through secondary pyrolysis reactions.
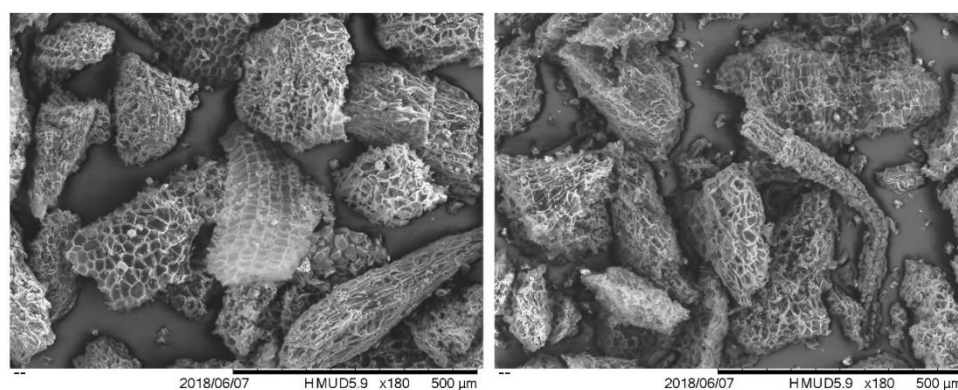

Figure 6. SEM micrographs of G-char biochar (**left**), and I-char (**right**).

3.5. Fuel Properties and Application of Cork Biochars

The biochars are charcoals mainly applied for soil amendment, but the fuel applications of these materials are also frequently referenced [29]. These applications such as co-combustion of biochars with coal require a specific set of calorific value, ash, fixed and volatile carbon content, and humidity in the biochars [29]. Among these criteria, the ash content may be the main obstacle for the fuel applications of cork derived chars, because the lignocellulosic pellets require an ash limit lower than 3 % according to prEN 14961-2 standard.

The proximate analysis is a useful technique to evaluate the fuel properties and stability of biochars [29]. It may also be used to study the extent of pyrolysis reaction, because the change in the fixed carbon (FC) content is related to the intensity of the pyrolysis treatment [30]. The results of the proximate analysis are shown in Figure 7. The results indicate that the pyrolysis reaction resulted in a significant decrease in the volatile content (VM) in both isothermal (I-Char) and non-isothermal (G-Char) biochars, and consequently in an increase in fixed carbon (FC) and ash contents leading to an increased fuel ratio (FR, ratio of fixed carbon/volatile matter).
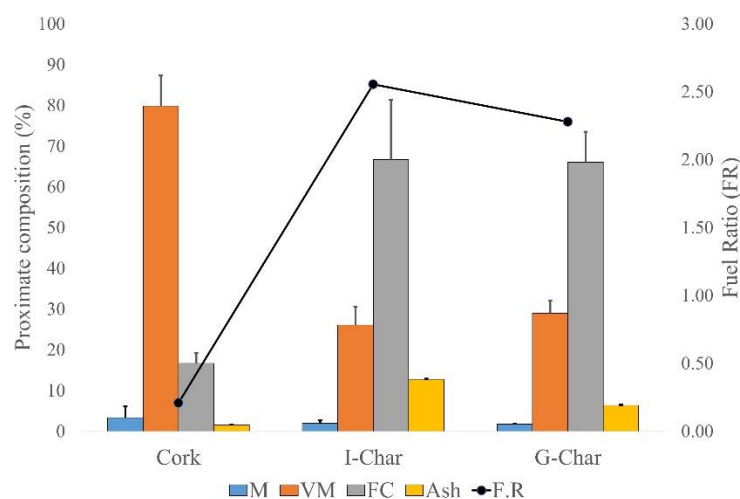
Figure 7. The proximate composition (M: moisture, VM: volatile matter, FC: fixed carbon, Ash: inorganic matter), and the fuel ratio (F.R) of cork and cork biochars.

It is noteworthy that, although the fuel ration is similar for both chars, the ash content seems to be lower in the non-isothermal one.

The cork biochars were also evaluated for their elemental composition and higher heating values, as shown in Table 2. The non-isothermal biochars contained higher amounts of carbon and lower amounts of hydrogen and oxygen compared to untreated cork, but also to the isothermal biochar.

Table 2. Results of elemental analysis (%, ash-free basis), H/C and O/C atomic ratios, and higher heating values (HHV, MJ kg^{-1}).

|	**Raw Cork**	**I-Char**	**G-Char**
C	53.8	63.5	71.5
H	6.5	5.3	3.6
O	39.7	31.2	24.9
O/C	0.55	0.37	0.26
H/C	1.44	0.99	0.60
HHV	19.7	21.3	22.8

The H/C and O/C atomic ratios in the raw material and biochars may be compared in Table 2. The atomic ratios of the non-isothermal biochar showed clear differences to

those of raw cork and the isothermal biochar. The elemental analysis suggests that the isothermal and non-isothermal biochars are similar to peat-like fuels [31]. The higher heating values show that non-isothermal biochars had slightly higher calorific value than isothermal biochars.

The *Quercus cerris* cork fractionated from the bark is not a homogeneous material. It has a chemical composition that may vary depending on the residual phloem content. Therefore, some of the differences in biochar properties might be allocated to differences in the composition of the used samples. Although both biochars have similar fuel properties, it seems that the biochars produced by the non-isothermal procedure have improved qualities when compared to those produced by the isothermal procedure.

The thermogravimetric analysis of the combustion of raw cork and non-isothermal biochar shows an increased thermal resistance to combustion in the biochars as evidenced by the shift of TG curves to higher temperatures (Figure 8). The isothermal biochars were more resistant to combustion when compared to non-isothermal biochars.
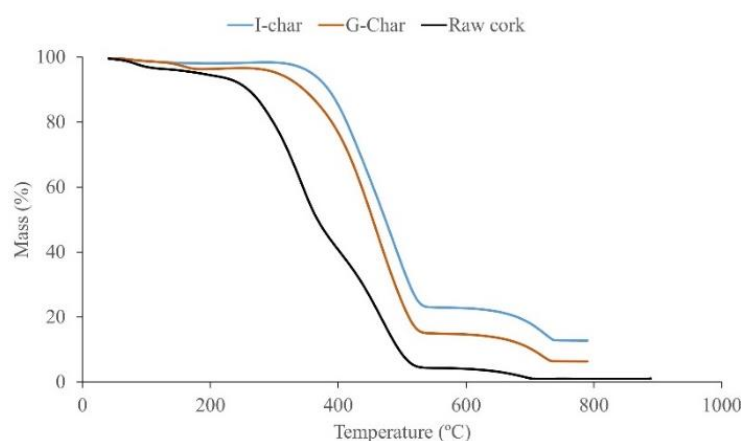

Figure 8. Combustion patterns of raw cork and non-isothermal biochars (G-char).

### 3.6. Hydrocarbon Composition of Cork Bio-Oil and Pyrolysis Gas

The pyrolysis of biomass generates, in addition to biochar, important amounts of condensate and gas products. The pyrolysis condensates are composed of oxygenated compounds such as alcohols, carboxylic acids, aldehydes, ketones, phenols, and water [32]. The raw pyrolysis condensates are not used directly because of their high water content, acidity, and viscosity but they may be converted and used after an upgrading process such as hydro-treating, catalytic cracking, esterification, or gasification [33].

The hydrocarbon composition of the pyrolysis condensate bio-oils is shown in Figures 9 and 10. The results indicate that the hydrocarbon fraction of pyrolysis condensates are composed mainly of aromatic C_5–C_{12} hydrocarbons. They are possibly lignin-derived compounds [34]. C_8 hydrocarbons were the main fraction followed by C_6 hydrocarbons in isothermal pyrolysis, while in non-isothermal pyrolysis the main fraction was C_{12} hydrocarbons. The composition of bio-oils also varied along the reactor length, i.e., in the top part of the reactor C_7 hydrocarbons predominate while in the bottom C_8 hydrocarbons constitute the main bio-oil fraction (data not shown). Interestingly, non-isothermal and isothermal pyrolysis resulted in different hydrocarbon compositions (Figures 9 and 10). Possibly, higher-chain hydrocarbons (C_{10}–C_{12}) crack in the isothermal pyrolysis to form lower-chain hydrocarbons.

The hydrocarbons present in the pyrolysis gas are in relatively low concentration and mainly composed of 2 carbon atom compounds (Figure 11). Because of the low amount of hydrocarbons present, it was not possible to calculate the exact amount of hydrocarbons in the pyrolysis gas.
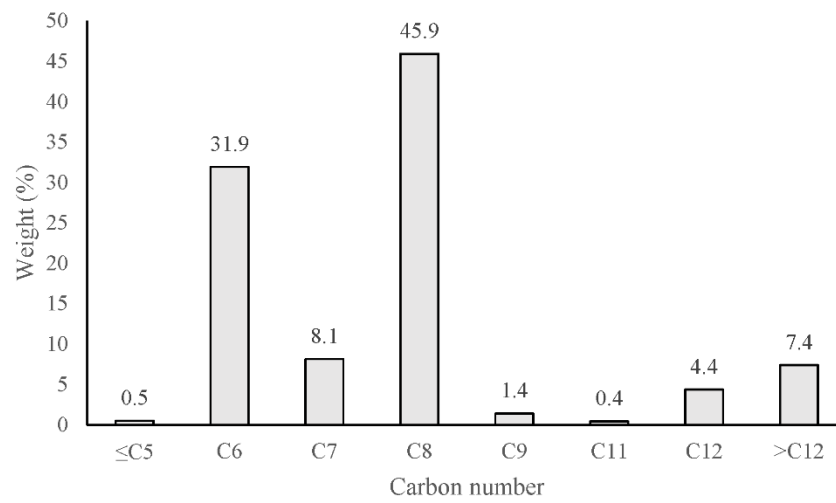
Figure 9. Hydrocarbon composition (by number of carbons) of isothermal pyrolysis condensate.
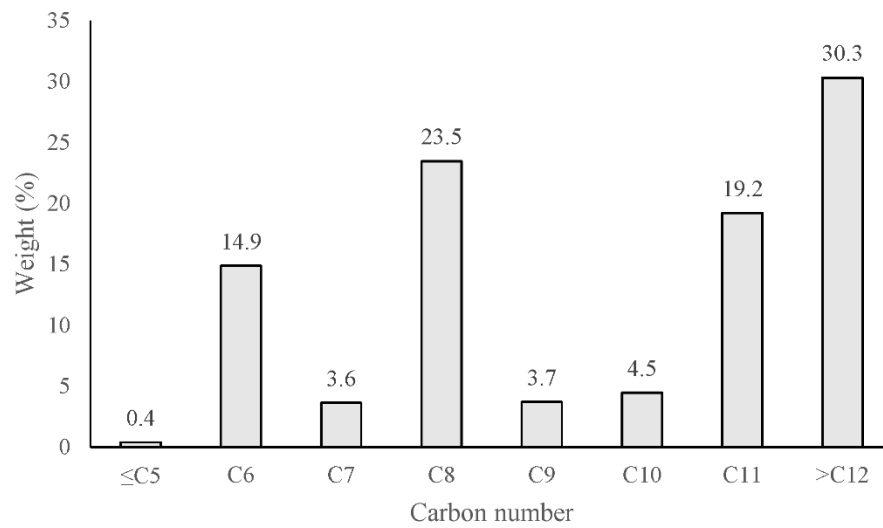
Figure 10. Hydrocarbon composition (by number of carbons) of non-isothermal pyrolysis condensate.
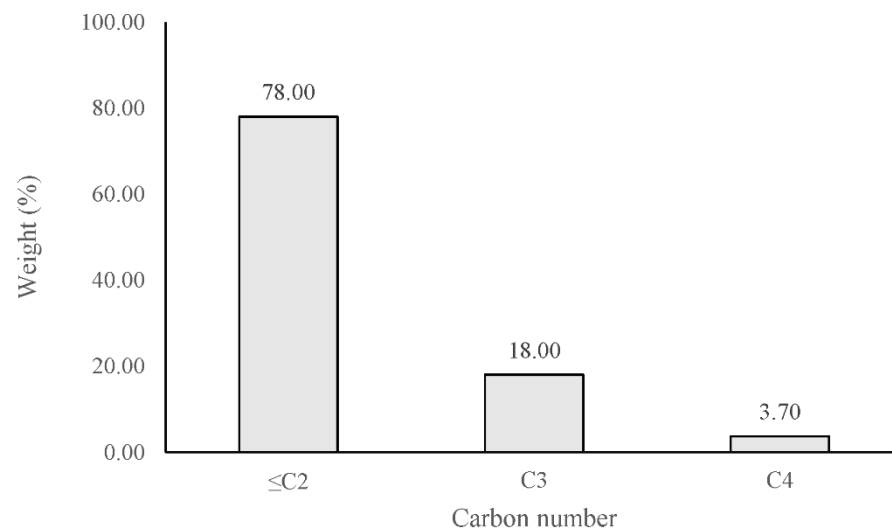
Figure 11. Hydrocarbon composition (by number of carbons) of isothermal pyrolysis gas.

4. Discussion

The pyrolysis conditions of lignocellulosic biomass may be tuned to obtain a certain product mix and achieve energy savings. An example of this tuning may be by using the torrefaction severity indexes which showed that the use of high temperature-short residence time combinations allows energy saving while obtaining the same char yield from biomass [35,36]. The similar char yields found in the present study in isothermal and non-isothermal conditions suggests that the actual temperature profile does not play an important role in the slow pyrolysis of cork and the non-isothermal pyrolysis is a less energy demanding way to produce biochars from cork.

Although the thermal degradation properties of cork are commercially exploited in the production of black (expanded) agglomerate insulation materials, the slow pyrolysis studies on cork are still scant [37–40]. The biochar yields of cork both in isothermal and non-isothermal slow pyrolysis conditions seem similar to those of other lignocellulosic biomass types [33,41]. Obviously, more data are needed for a comprehensive characterization of the slow pyrolysis of cork. Our results suggest that the biochar yield from cork is mainly dependent on the final pyrolysis temperature and the heat transfer rate. The similar biochar yields under the conventional isothermal and non-isothermal conditions imply that slow pyrolysis of cork under non-isothermal conditions is a promising method in terms of cost reduction because expensive heating is not required after the final pyrolysis temperature is reached.

It is possible to see a sharp endothermic peak right after the sample is introduced in Figures 3 and 4 (when the oven temperature reaches 500 °C). This endothermic process corresponds to the heating of the sample, to moisture evaporation, as well as to some endothermic reactions. However, as time progresses the heat flow shifts to exothermic and a slight exothermic value, corresponding to higher temperatures in the reactor with the sample than in the blank experiment, throughout the remaining time. In fact, at the end of the run, the temperature in the reactor containing samples is still significantly higher than the temperature of the oven itself, indicating heat generation inside the reactor.

The FT-IR observations indicate that there is extensive decarboxylation involved in the degradation of cellulose and hemicelluloses. An interesting peak appears at 1411 cm^{-1} which was more intense in isothermal char and assigned to the aromatic C=C stretching vibration [42,43], indicating the initiation of aromatization in the biochar structure. The cellular expansion in the non-isothermal biochars was also higher suggesting that these materials may be more efficiently used for soil amendment [44,45]. The cork cells remained intact even after exposure to high temperatures. This property is related to the resilient cellular structure and chemical composition of cork [46].

Regarding the non-fuel uses, the cork biochars may be used as adsorbents or soil amendment materials. In order to evaluate the adsorption properties of biochars, the elemental composition is also relevant. The lower O/C ratio of non-isothermal biochars indicates that they are more hydrophobic than the raw material and isothermal biochars. These results suggest that non-isothermal biochars might be applied as adsorbents of non-polar substances, while isothermal biochars may be used as adsorbents of aqueous effluents [47]. The high ash content of non-isothermal and isothermal biochars might also be used to produce activated carbons or hierarchical activated carbons to be used for adsorption of heavy metals or they can be used as electrode materials [37,48]. For the soil amendment applications, the non-isothermal and isothermal biochars with cellular structure and high fixed carbon contents showed a promising potential as evidenced by SEM observations and proximate analysis results [49,50]. The biochars are also sources of nutrients for plant growth. Particularly high-ash-containing biochars are potential nutrient sources such as of phosphorus [51].

The hydrocarbon composition of cork condensates after non-isothermal and isothermal pyrolysis suggests that they may be upgraded using either gasification or hydrotreatment routes to produce liquid fuels, although this was not the subject of this study. In fact, the bio-oil to gasoline route is reported as the most-widely used technique for bio-oils

upgrading [32]. It is well-known that pyrolysis gas of lignocellulosic biomass is composed mainly of CO, CO2, CH4, H2, and H2O and light hydrocarbons and the gas composition depends mainly on the pyrolysis temperature [52,53]. However, the pyrolysis gas may be used to produce heat for the pyrolysis process or to produce Fischer–Tropsch hydrocarbons, methanol, or ethanol through syngas conversion [7,53,54]. In fact, in the last years, there has been a surge of interest in producing hydrogen from pyrolysis gas through dry and steam reforming or water–gas shift reactions [55,56].

5. Conclusions

The slow pyrolysis of *Quercus cerris* cork under isothermal and non-isothermal conditions was shown to be an effective method to produce value-added biochars as well as bio-oil and gas products. The following specific conclusions can be drawn from the study.

1. The slow pyrolysis of *Quercus cerris* cork results in approximately 32% biochars, 18% condensates, and 50% pyrolysis gas.
2. Cork undergoes a slightly exothermic process during slow pyrolysis, possibly associated with decarboxylation reactions, which reduces the required amount of external heat.
3. Cork suberin undergoes degradation during slow pyrolysis.
4. Decarboxylation and aromatization occur in cork pyrolysis, most noticeably under isothermal conditions.
5. The hydrocarbon fraction of cork bio-oil consists of C_5–C_{12} compounds with C_8 compounds making the main fraction. The hydrocarbon fraction of the cork pyrolysis gas is composed mainly of C_1–C_2 compounds.
6. The non-isothermal pyrolysis is a promising method for producing biochars at a lower cost than isothermal pyrolysis.

References

1. Kamm, B.; Kamm, M.; Gruber, P.R.; Kromus, S. Biorefinery systems–An overview. Biorefineries-Industrial Process. In *Biorefineries-Industrial Processes and Products: Status Quo and Future Directions*; John Wiley & Sons, Inc.: Hoboken, NJ, USA, 2005; pp. 1–40.
2. Cherubini, F. The biorefinery concept: Using biomass instead of oil for producing energy and chemicals. *Energy Convers. Manag.* **2010**, *51*, 1412–1421. [CrossRef]
3. Demirbaş, A.; Ozturk, T.; Demirbas, M.F. Recovery of Energy and Chemicals from Carbonaceous Materials. *Energy Sources Part A Recover. Util. Environ. Eff.* **2006**, *28*, 1473–1482. [CrossRef]
4. Bain, R.L.; Broer, K. *Gasification*; National Renewable Energy Lab. (NREL): Golden, CO, USA, 2011.
5. Dahmen, N.; Henrich, E.; Dinjus, E.; Weirich, F. The bioliq®bioslurry gasification process for the production of biosynfuels, organic chemicals, and energy. *Energy Sustain. Soc.* **2012**, *2*, 3. [CrossRef]
6. Bridgwater, T. Challenges and Opportunities in Fast Pyrolysis of Biomass: Part I. *Johns. Matthey Technol. Rev.* **2018**, *62*, 118–130. [CrossRef]
7. Bridgwater, A.V.; Peacocke, G.V.C. Fast pyrolysis processes for biomass. *Renew. Sustain. Energy Rev.* **2000**, *4*, 1–73. [CrossRef]

8. Brown, T.R.; Wright, M.M.; Brown, R.C. Estimating profitability of two biochar production scenarios: Slow pyrolysis vs fast pyrolysis. *Biofuels Bioprod. Biorefining* **2011**, *5*, 54–68. [CrossRef]

9. Pasztory, Z.; Mohácsiné, I.R.; Gorbacheva, G.; Börcsök, Z. The utilization of tree bark. *BioResources* **2016**, *11*, 7859–7888. [CrossRef]

10. Tran, D.Q.; Rai, C. A kinetic model for pyrolysis of Douglas fir bark. *Fuel* **1978**, *57*, 293–298. [CrossRef]

11. Fengel, D.; Wegener, G. Wood: Chemistry, ultrastructure. *Reactions* **1984**, *613*, 1960–1982.

12. Sjöström, E. *Wood Chemistry: Fundamentals and Applications*; Gulf Professional Publishing: San Diego, CA, USA, 1993; ISBN 0-12-647481-8.

13. Leite, C.; Pereira, H. Cork-containing barks—A review. *Front. Mater.* **2017**, *3*, 63. [CrossRef]

14. Şen, A.; Miranda, I.; Santos, S.; Graça, J.; Pereira, H. The chemical composition of cork and phloem in the rhytidome of Quercus cerris bark. *Ind. Crop. Prod.* **2010**, *31*, 417–422. [CrossRef]

15. Şen, A.; Leite, C.; Lima, L.; Lopes, P.; Pereira, H. Industrial valorization of Quercus cerris bark: Pilot scale fractionation. *Ind. Crop. Prod.* **2016**, *92*, 42–49. [CrossRef]

16. Şen, A.; Miranda, I.; Ferreira, J.; Lourenço, A.; Pereira, H. Chemical composition and cellular structure of ponytail palm (Beaucarnea recurvata) cork. *Ind. Crop. Prod.* **2018**, *124*, 845–855. [CrossRef]

17. Strandberg, M.; Olofsson, I.; Pommer, L.; Wiklund-Lindström, S.; Åberg, K.; Nordin, A. Effects of temperature and residence time on continuous torrefaction of spruce wood. *Fuel Process. Technol.* **2015**, *134*, 387–398. [CrossRef]

18. Wilhelm, A.; Hedden, K. A non-isothermal experimental technique to study coal extraction with solvents in liquid and supercritical state. *Fuel* **1986**, *65*, 1209–1215. [CrossRef]

19. Di Blasi, C.; Branca, C.; Galgano, A. On the Experimental Evidence of Exothermicity in Wood and Biomass Pyrolysis. *Energy Technol.* **2017**, *5*, 19–29. [CrossRef]

20. Chaiwat, W.; Hasegawa, I.; Tani, T.; Sunagawa, K.; Mae, K. Analysis of Cross-Linking Behavior during Pyrolysis of Cellulose for Elucidating Reaction Pathway. *Energy Fuels* **2009**, *23*, 5765–5772. [CrossRef]

21. Şen, A.; Marques, A.V.; Gominho, J.; Pereira, H. Study of thermochemical treatments of cork in the 150–400°C range using colour analysis and FTIR spectroscopy. *Ind. Crop. Prod.* **2012**, *38*, 132–138. [CrossRef]

22. Nobre, C.; Şen, A.; Durão, L.; Miranda, I.; Pereira, H.; Gonçalves, M. Low-temperature pyrolysis products of waste cork and lignocellulosic biomass: Product characterization. *Biomass Convers. Biorefinery* **2021**, 1–11. [CrossRef]

23. Longo, A.; Nobre, C.; Sen, A.; Panizio, R.; Brito, P.; Gonçalves, M. Torrefaction Upgrading of Heterogenous Wastes Containing Cork and Chlorinated Polymers. *Environments* **2022**, *9*, 99. [CrossRef]

24. Şen, A.U.; Fonseca, F.G.; Funke, A.; Pereira, H.; Lemos, F. Pyrolysis kinetics and estimation of chemical composition of Quercus cerris cork. *Biomass Convers. Biorefinery* **2020**, *12*, 4835–4845. [CrossRef]

25. Frost, R.L.; Yang, J.; Ding, Z. Raman and FTIR spectroscopy of natural oxalates: Implications for the evidence of life on Mars. *Chin. Sci. Bull.* **2003**, *48*, 1844–1852. [CrossRef]

26. Wulandari, W.T.; Rochliadi, A.; Arcana, I.M. Nanocellulose prepared by acid hydrolysis of isolated cellulose from sugarcane bagasse. In Proceedings of the IOP Conference Series: Materials Science and Engineering; IOP Publishing: Solo, Indonesia, 2015; Volume 107, p. 12045.

27. Kubo, S.; Kadla, J.F. Hydrogen Bonding in Lignin: A Fourier Transform Infrared Model Compound Study. *Biomacromolecules* **2005**, *6*, 2815–2821. [CrossRef]

28. Wei, L.; Agarwal, U.P.; Hirth, K.C.; Matuana, L.M.; Sabo, R.C.; Stark, N.M. Chemical modification of nanocellulose with canola oil fatty acid methyl ester. *Carbohydr. Polym.* **2017**, *169*, 108–116. [CrossRef]

29. Aller, D.; Bakshi, S.; Laird, D.A. Modified method for proximate analysis of biochars. *J. Anal. Appl. Pyrolysis* **2017**, *124*, 335–342. [CrossRef]

30. Ronsse, F.; van Hecke, S.; Dickinson, D.; Prins, W. Production and characterization of slow pyrolysis biochar: Influence of feedstock type and pyrolysis conditions. *GCB Bioenergy* **2013**, *5*, 104–115. [CrossRef]

31. Basu, P. *Biomass Gasification and Pyrolysis: Practical Design and Theory*; Academic Press: Burlington, MA, USA, 2010; ISBN 0080961622.

32. Galadima, A.; Muraza, O. In situ fast pyrolysis of biomass with zeolite catalysts for bioaromatics/gasoline production: A review. *Energy Convers. Manag.* **2015**, *105*, 338–354. [CrossRef]

33. Bridgwater, A. V Review of fast pyrolysis of biomass and product upgrading. *Biomass Bioenergy* **2012**, *38*, 68–94. [CrossRef]

34. Marques, A.V.; Pereira, H. Aliphatic bio-oils from corks: A Py–GC/MS study. *J. Anal. Appl. Pyrolysis* **2014**, *109*, 29–40. [CrossRef]

35. Chen, W.-H.; Huang, M.-Y.; Chang, J.-S.; Chen, C.-Y. Thermal decomposition dynamics and severity of microalgae residues in torrefaction. *Bioresour. Technol.* **2014**, *169*, 258–264. [CrossRef]

36. Chen, W.-H.; Cheng, C.-L.; Show, P.-L.; Ong, H.C. Torrefaction performance prediction approached by torrefaction severity factor. *Fuel* **2019**, *251*, 126–135. [CrossRef]

37. Wang, Q.; Lai, Z.; Mu, J.; Chu, D.; Zang, X. Converting industrial waste cork to biochar as Cu (II) adsorbent via slow pyrolysis. *Waste Manag.* **2020**, *105*, 102–109. [CrossRef] [PubMed]

38. Pereira, H. The thermochemical degradation of cork. *Wood Sci. Technol.* **1992**, *26*, 259–269. [CrossRef]

39. Marques, A.V.; Pereira, H.; Meier, D.; Faix, O. Quantitative analysis of cork (Quercus suber L.) and milled cork lignin by FTIR spectroscopy, analytical pyrolysis, and total hydrolysis. *Holzforschung-Int. J. Biol. Chem. Phys. Technol. Wood* **1994**, *48*, 43–50. [CrossRef]

40. Fernandes, E.M.; Correlo, V.M.; Mano, J.F.; Reis, R.L. Cork–polymer biocomposites: Mechanical, structural and thermal properties. *Mater. Des.* **2015**, *82*, 282–289. [CrossRef]

41. Duman, G.; Okutucu, C.; Ucar, S.; Stahl, R.; Yanik, J. The slow and fast pyrolysis of cherry seed. *Bioresour. Technol.* **2011**, *102*, 1869–1878. [CrossRef]

42. Pituello, C.; Francioso, O.; Simonetti, G.; Pisi, A.; Torreggiani, A.; Berti, A.; Morari, F. Characterization of chemical–physical, structural and morphological properties of biochars from biowastes produced at different temperatures. *J. Soils Sediments* **2015**, *15*, 792–804. [CrossRef]

43. Nan, H.; Yin, J.; Yang, F.; Luo, Y.; Zhao, L.; Cao, X. Pyrolysis temperature-dependent carbon retention and stability of biochar with participation of calcium: Implications to carbon sequestration. *Environ. Pollut.* **2021**, *287*, 117566. [CrossRef]

44. Şen, A.U.; Nobre, C.; Durão, L.; Miranda, I.; Pereira, H.; Gonçalves, M. Low-temperature biochars from cork-rich and phloem-rich wastes: Fuel, leaching, and methylene blue adsorption properties. *Biomass Convers. Biorefinery* **2020**, *12*, 3899–3909. [CrossRef]

45. Şen, A.U.; Pereira, H. State-of-the-Art Char Production with a Focus on Bark Feedstocks: Processes, Design, and Applications. *Processes* **2021**, *9*, 87. [CrossRef]

46. Pereira, H. Chapter 13—Cork agglomerates and composites. In *Cork*; Pereira, H., Ed.; Elsevier Science B.V.: Amsterdam, The Netherlands, 2007; pp. 289–303. ISBN 978-0-444-52967-1.

47. Sun, Y.; Gao, B.; Yao, Y.; Fang, J.; Zhang, M.; Zhou, Y.; Chen, H.; Yang, L. Effects of feedstock type, production method, and pyrolysis temperature on biochar and hydrochar properties. *Chem. Eng. J.* **2014**, *240*, 574–578. [CrossRef]

48. Jin, H.; Wang, X.; Gu, Z.; Polin, J. Carbon materials from high ash biochar for supercapacitor and improvement of capacitance with HNO3 surface oxidation. *J. Power Sources* **2013**, *236*, 285–292. [CrossRef]

49. Enders, A.; Hanley, K.; Whitman, T.; Joseph, S.; Lehmann, J. Characterization of biochars to evaluate recalcitrance and agronomic performance. *Bioresour. Technol.* **2012**, *114*, 644–653. [CrossRef] [PubMed]

50. Lehmann, J.; Joseph, S. *Biochar for Environmental Management: Science, Technology and Implementation*; Routledge: London, UK, 2015; ISBN 1134489536.

51. Wang, T.; Camps-Arbestain, M.; Hedley, M.; Bishop, P. Predicting phosphorus bioavailability from high-ash biochars. *Plant Soil* **2012**, *357*, 173–187. [CrossRef]

52. Heo, H.S.; Park, H.J.; Park, Y.-K.; Ryu, C.; Suh, D.J.; Suh, Y.-W.; Yim, J.-H.; Kim, S.-S. Bio-oil production from fast pyrolysis of waste furniture sawdust in a fluidized bed. *Bioresour. Technol.* **2010**, *101*, S91–S96. [CrossRef] [PubMed]

53. Shabangu, S.; Woolf, D.; Fisher, E.M.; Angenent, L.T.; Lehmann, J. Techno-economic assessment of biomass slow pyrolysis into different biochar and methanol concepts. *Fuel* **2014**, *117*, 742–748. [CrossRef]

54. Swanson, R.M.; Platon, A.; Satrio, J.A.; Brown, R.C. Techno-economic analysis of biomass-to-liquids production based on gasification. *Fuel* **2010**, *89*, S11–S19. [CrossRef]

55. Uddin, N.; Daud, W.W.; Abbas, H.F. Potential hydrogen and non-condensable gases production from biomass pyrolysis: Insights into the process variables. *Renew. Sustain. Energy Rev.* **2013**, *27*, 204–224. [CrossRef]

56. Xu, X.; Jiang, E.; Wang, M.; Xu, Y. Dry and steam reforming of biomass pyrolysis gas for rich hydrogen gas. *Biomass-Bioenergy* **2015**, *78*, 6–16. [CrossRef]